Magnetic characterization of magnetic tunnel junction devices using circle transfer curves

N. S. Safron,[1,2] B. D. Schrag,[1,a)] Xiaoyong Liu,[1] Weifeng Shen,[1,2] D. Mazumdar,[2] M. J. Carter,[1] and Gang Xiao[2]
[1]*Micro Magnetics, Inc., 421 Currant Road, Fall River, Massachusetts 02720, USA*
[2]*Department of Physics, Brown University, 182 Hope Street, Providence, Rhode Island 02912, USA*

(Received 9 September 2007; accepted 27 November 2007; published online 5 February 2008)

We describe new characterization methods that allow an accurate determination of all of the magnetic parameters that govern the behavior of magnetoresistive devices. These characterization methods are explained and used to measure the magnetic properties of MgO-based magnetic tunnel junction (MTJ) devices with magnetoresistance values of over 150%. We will show that the analysis of so-called "circle transfer curves," which are measurements of the device magnetoresistance in a rotating, constant-magnitude applied field, can accurately determine the magnitude and direction of the free layer anisotropy as well as the pinned layer orientation and exchange bias strength. We also show how a measurement of the MTJ's remnant resistance curve, obtained by saturating the MTJ at different field angles and then removing the applied field, can provide additional information on the free layer anisotropy characteristics. We will also compare our results with values extracted from traditional Stoner-Wohlfarth asteroid curves. Finally, we show that the extracted parameters can accurately predict the shape of traditional MTJ transfer curves. © *2008 American Institute of Physics*. [DOI: 10.1063/1.2837115]

I. INTRODUCTION

Magnetic tunnel junction (MTJ) devices have been the subject of intense study since the first observations of large room-temperature magnetoresistance in these structures.[1–3] Industrial research into the fabrication of MTJ structures has targeted two major applications areas for these devices. The first is for nonvolatile magnetic memory technologies, where each MTJ cell is used to store a single bit of data.[4] The other application of MTJ devices is as magnetic field sensors (for example, as part of the read/write heads used in the hard disk industry).[5,6] The recent discovery of very large magnetoresistance ratios in MTJ devices with MgO tunnel barriers has enhanced the industrial potential of this technology.[7–9]

An accurate method for measuring the governing properties of MTJs is essential to understanding the physics occurring in these devices. Understanding the basic parameters that determine how the resistance of a MTJ cell varies in an arbitrary applied field is critical, both from a fundamental and an applications point of view. For example, the creation of an ideal MTJ low-field sensor requires that the MTJ be fabricated with little to no magnetic hysteresis. A number of different methods have been proposed to eliminate the hysteretic effects of MTJ sensors. The linearization of spin-valve-type MTJ field sensors has generally been accomplished via one of two common methods: (1) the application of applied magnetic fields perpendicular to the anisotropy (easy) axis of the MTJ film[5,10] and (2) attempts to rotate the free layer anisotropy so that it is perpendicular to the pinned layer magnetization.[11,12] Before either of these methods can be implemented, the anisotropy characteristics of the free and pinned layers must be accurately measured. Knowledge of these parameters is also very important for scientists and engineers who are involved in implementing fabrication processes used for the mass production of MTJ or GMR devices.

Even after over a decade of research, there is no satisfactory method to measure all the physical parameters that govern the behavior of MTJs. Magnetometry methods can only measure bulk films or devices with relatively large magnetic volumes. Therefore, they cannot measure the variation or uniformity of parameters across a wafer, nor can they measure the shape-dependent behavior (e.g., anisotropy, magnetostatic coupling) of single microscopic devices. Traditional resistance-versus-field transfer curves can measure coercive fields, but cannot adequately determine the absolute magnetic orientation of either MTJ electrode. Additionally, data obtained in this manner can be skewed by small errors in the pinned layer orientation or by effective offset fields (i.e., those caused by Néel or magnetostatic coupling).[13] The use of Stoner-Wohlfarth (S-W) "asteroid" curves can give estimates of the easy- and hard-axis bias fields[14] and can estimate the anisotropy parameters, but asteroid curves almost always show significant deviations from theoretical predictions, due to noncoherent switching events caused by domain-wall motion and nucleation.[15,16] This complicates interpretation of the results, as does the observed "stretching" of most experimentally determined asteroid curves.[14,17] Asteroid curves are also unable to provide quantitative information about the properties of the pinned layer. In addition, all of these traditional characterization methods become even more suspect when attempting to understand the behavior of individual, micron-size (or smaller) MTJ elements.

In this work, we describe new methods for measuring

a)Author to whom correspondence should be addressed. Electronic mail: schrag@micromagnetics.com.

the most important physical parameters that control the behavior of MTJ (or GMR) spin-valve devices. We will show how the use of sets of so-called "circle transfer curves" can be analyzed to yield all of the information needed to predict the behavior of our MTJ devices under an arbitrary two-dimensional applied field. In particular, we can use the circle transfer curve data to accurately extract the strength and direction of the free layer's uniaxial anisotropy, the angular orientation of the pinned electrode, and the effective exchange field felt by the pinned layer.

These circle transfer curves, which are simply measurements of the device resistance as a function of the applied field angle, measured with a fixed field strength, have several advantages over other techniques. First, because the circle transfer curves are measured at field strengths much greater than the anisotropy strength of the free layer, circle transfer curves measure the behavior of the MTJ only in the coherent regime. Whereas asteroid curves are based on measuring the details of the irreversible magnetic switching events of the free layer of the MTJ, these curves avoid the often complicated and unpredictable switching processes entirely. Second, these circle curves can yield quantitative information about the magnetic state of the pinned layer,[18] information that is not directly available from the asteroid data. Finally, while the measurement of an asteroid curve might require from 20 to 50 field sweeps, only three circle transfer curves are needed to extract the desired information about the junction. Therefore, this new method has the potential to be much faster.

We will demonstrate how these circle transfer curves have been used to determine the magnetic parameters of many MgO-based magnetic tunnel junction devices. We will show that our results are in good agreement with data extracted from standard asteroid curves. We also demonstrate that our anisotropy data are in excellent agreement with data obtained from so-called "remnant resistance curves." These curves are a straightforward way to measure the anisotropy characteristics of the MTJ's free layer, by saturating it in a field at an arbitrary angle and then allowing it to relax by removing the field.[19,20] Analysis of the remnant resistance data can give information about the free layer's anisotropy orientation and dispersion. Finally, we will show that the parameters extracted from the circle curve data can be used to very accurately predict the standard transfer curve behavior of the MTJ device. This last result also demonstrates that the coherent behavior of our MTJ devices can be reasonably approximated by the single-particle S-W model, which we use as the basis of our analysis.

II. SAMPLE DETAILS

The layer structure of the devices studied was (thicknesses in Å) 50 Ta/300 Ru/50 Ta/20 CoFe/150 IrMn/20 CoFe/8 Ru/30 CoFeB/15 MgO/120 CoFeB/20 Ta/20 Ru. Here, the CoFe/Ru/CoFeB trilayer just above the MgO insulating barrier is a synthetic antiferromagnetic (SAF) free layer, which we have chosen based on its superior magnetic characteristics (reduced magnetic coupling). The MTJs were deposited on thermally oxidized silicon substrates in an applied magnetic field of 120 Oe using dc and rf magnetron sputtering. The wafers were then patterned into individual junctions via ion-beam etching, with individual junctions having varying aspect ratios and dimensions of $4-45$ μm. More details regarding the sample fabrication are available elsewhere.[9]

The ultimate goal of our work is to design improved methods for fabricating junctions in the sensor orientation, which is characterized by MTJ devices whose pinned and free layer orientations are perpendicular in small applied fields. In general, the standard high-temperature annealing process used for MgO-based MTJ devices leaves the pinned layer orientation and free layer anisotropy axis parallel. The resulting devices are ideal for MRAM applications but are not suitable for sensor devices. Therefore, one of the samples that we studied was subjected to a two-step annealing process, whereby the sample was annealed twice at high temperature: first with an applied field perpendicular to the as-deposited field and then parallel to it. Both annealing steps were done at 375 °C for 45 min. The theory behind this two-step process was that the first annealing would serve to crystallize the MgO barrier, permanently setting the free layer's anisotropy direction, and that the second annealing could then rotate the pinned layer direction simply by resetting the exchange bias direction. We will demonstrate how these new characterization methods were vitally important in understanding the physical and magnetic effects of this two-step annealing process.

III. CIRCLE TRANSFER CURVES

The circle curve is a simple concept: the device resistance is recorded as a function of the applied field angle, as the field angle is rotated with a constant magnitude. Making this measurement requires no new machinery beyond what is needed for asteroid measurements, and the measurement of the handful of circle curves that are generally needed is much quicker than the acquisition of a full asteroid curve. The circle curve also has the advantage over standard transfer curves of being able to more accurately determine the true magnetoresistance of the sample, as it guarantees that the true parallel and antiparallel states of the junction are reached. A diagram showing the details of the measurement techniques we used in this work, including the circle curve, is shown in Fig. 1.

For analysis, the resistance measurements are first converted to conductance data. The data from several (three to ten) circle curves are all fitted based on a S-W model,[21] which has six adjustable parameters in the most general case: the magnitude (H_K) and angle (θ_K) of the free layer's uniaxial anisotropy term, the exchange bias direction (θ_E) and effective strength (H_E), and the internal offset fields in the two in-plane directions (H_{0X} and H_{0Y}). The purpose of including the pinned layer field strength is to allow the pinned layer to rotate slightly from the exchange bias direction as a result of the applied external field H, according to the following relation:

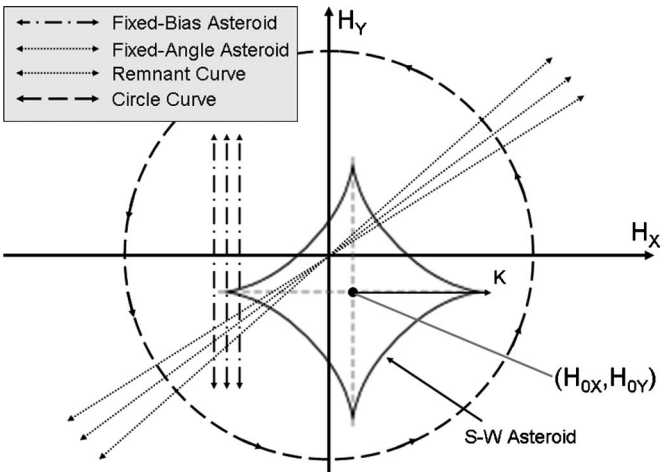

FIG. 1. Schematic showing some details about how the different measurement techniques are conducted in two-dimensional field space. A Stoner-Wohlfarth asteroid curve is also shown, with its origin shifted from the field-space origin due to internal offset fields (H_{0X} and H_{0Y}).

$$\theta_P = \tan^{-1}\left(\frac{H_E \sin\ \theta_E + H \sin\ \theta_H}{H_E \cos\ \theta_E + H \cos\ \theta_H}\right). \tag{1}$$

The free layer magnetization angle θ_F is calculated by finding the angular orientation, which minimizes its S-W free energy:

$$E(\theta) = -H\cos(\theta - \theta_H) + \frac{H_k}{2}\sin^2(\theta - \theta_K) - H_{0X}\cos\ \theta - H_{0Y}\sin\ \theta, \tag{2}$$

and the resulting MTJ conductance G is simply modeled as

$$G = G_0[1 + P^2\cos(\theta_F - \theta_P)], \tag{3}$$

where G_0 and P are fabrication parameters related to the resistance-area product, geometry, and overall magnetoresistance of the MTJ devices. Figure 2 summarizes some of the above parameters and provides a graphical representation of the model used to determine the behavior of both the free and pinned magnetic layers. The analysis of circle curves in this paper assumes coherent motion of the free electrode. This assumption is validated by the fact that circle curves measured in both rotational directions are always almost identical. A sample experimental circle curve, taken with a field strength of 130 G, is also shown in Fig. 3.

IV. REMNANT RESISTANCE CURVES

As outlined above, the remnant resistance curve is an attempt to focus on the anisotropy characteristics of the free layer. Variations of this type of measurement have been made for many years by different groups.[19,20,22] For a magnetic particle (or MTJ free layer) with a uniaxial anisotropy, there are two energy minima, with an angular separation of 180°, in which the junction can exist in zero field (ignoring, for the moment, offset fields). The true minimum at any given point in time is determined by the magnetic history of the junction. By applying a large field (sufficient to align the free layer with the field direction), and then relaxing the field to zero, the junction is forced to choose one of these two minima.

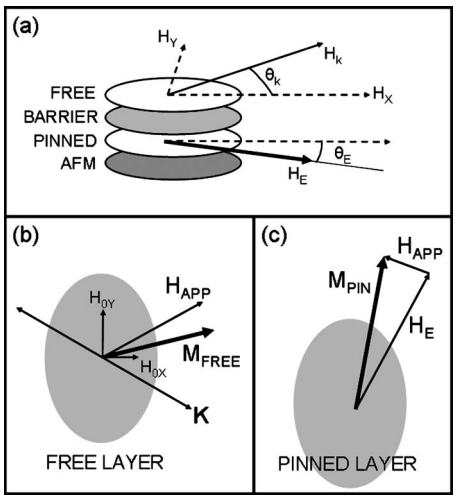

FIG. 2. (a) Schematic of the MTJ multilayer showing the relevant physical quantities that dictate the junction behavior. (b) Simplified model of the free layer, where the magnetization is determined by the two offset field components (H_{0X} and H_{0Y}), the sample's uniaxial anisotropy, and the external applied field (H_A). (c) Model of the pinned layer magnetization, which is assumed to be the vector sum of two forces: the applied field and the exchange biasing field (H_E).

Assuming an S-W particle, the junction will always prefer to relax to the minimum that makes the smallest angle with the applied field direction. The remnant resistance curve essentially measures the resistance of the MTJ at zero field, after this relaxation process is conducted, for all angles. We can therefore expect that an ideal S-W particle will have a remnant curve as shown in Fig. 3. This ideal curve will exhibit only two possible resistance values, and there will two sharp transitions between these two resistance states at the two angles that are exactly perpendicular to the anisotropy direction. We denote these angles θ_{J1} and θ_{J2}. The actual anisotropy direction is then given simply by the average of these two angles.

It is true that nonzero easy- and hard-axis offset fields

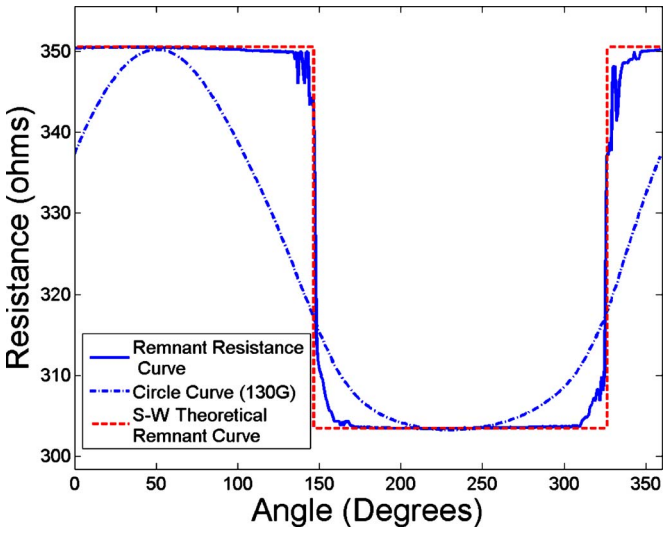

FIG. 3. (Color online) Examples of the raw data from a circle curve (taken at 130 G; dot-dashed line) and a remnant resistance curve (solid line), along with a theoretical remnant resistance curve (dashed line). The two sets of data were taken during the same set of field sweeps.

will perturb the results of this type of measurement. Rewriting the two offset fields H_{0X} and H_{0Y} in terms of their components parallel ($H_{\|}$) and perpendicular ($H_{\perp}$) to the anisotropy direction, we can use geometrical arguments to calculate that the expected deviation in the angular positions of the two jumps. To first order, these deviations are given by

$$\Delta\theta_{J1} = \tan^{-1}\left(\frac{H_{\|}}{H_K - H_{\perp}}\right),$$

$$\Delta\theta_{J2} = \tan^{-1}\left(\frac{-H_{\|}}{H_K + H_{\perp}}\right). \quad (4)$$

While these deviations are significant, the fact that we are averaging the two jump angles to calculate the anisotropy causes much of the deviation to drop out. The estimated error in the anisotropy angle based on the above deviations is then given by

$$\Delta\theta_K \cong \frac{H_{\|}H_{\perp}}{H_K^2 - H_{\perp}^2}. \quad (5)$$

As we will show, our junctions exhibit offset fields that are at least an order of magnitude smaller than their anisotropy strength. Therefore, we estimate that these offset fields will not create an error of more than a few degrees in our extracted values for θ_K. An example measured remnant resistance curve is given in Fig. 3. The shape of the curve is similar to what we expect, but, as expected, the two transitions are not infinitely sharp. The sharpness of these two transitions also contains information about the anisotropy distribution of the sample. In fact, it can easily be shown that the shape of the remnant resistance curve can also be used to estimate the dispersion of the free layer anisotropy.[19] Assuming that the sample can be considered an ensemble of noninteracting S-W particles with different anisotropy axes, the angular dispersion of anisotropy in the sample is simply proportional to the normalized derivative of the remnant curve.

V. ASTEROID CURVES

For all the asteroid measurements, we have used angle-dependent (or "fixed-angle") transfer curve data instead of the more common method (referred to as the "fixed-bias" method) of repeatedly applying a fixed field in one direction and then sweeping the orthogonal field component through a full transfer curve. Figure 1 shows a field-space representation of each of these processes. Our method measures the device resistance as a function of varying magnetic field strength at a fixed applied field angle. Each transfer curve is taken up to a maximum field strength of ± 40 Oe and transfer curves are acquired at 5° increments.

Acquiring the asteroid curve requires that each sweep be analyzed to extract two switching field values (one for the increasing field direction and one for decreasing field). In general, the switching field values are calculated by finding the point of largest derivative (dR/dH) in the measured transfer curve at each angle. In practice, we have found that all but a few of the angular sweeps for a given junction will exhibit a hysteretic jump, making this method quite reliable

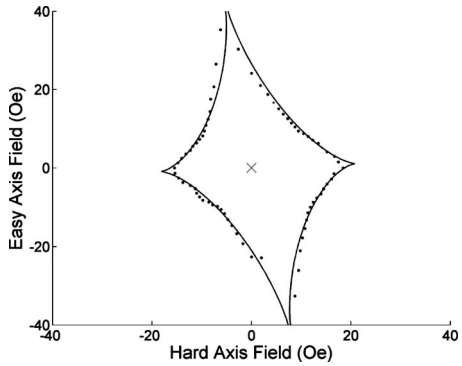

FIG. 4. Experimentally measured angle-dependent asteroid curve of a sample MTJ. Solid circles represent the data, while the solid line represents the best fit to the modified S-W model [Eq. (7)].

(with the exceptions being sweeps at field angles, which are nearly perpendicular to the anisotropy direction).

A sample experimentally measured asteroid curve is given in Fig. 4. The extracted results consist of the applied field at which switching events occur as a function of the applied external field angle. The switching field value extracted at each angle is the only information that is considered; the actual resistance values are not used for analysis once these values have been extracted. The switching fields are fitted to the theoretical model using a custom fitting algorithm based on a least-squares minimization process. A junction with a perfect S-W character, including offset fields, will have an asteroid that is described by

$$H(\theta) = H_K[\cos^{2/3}(\theta - \theta_K) + \sin^{2/3}(\theta - \theta_K)]^{-3/2} - H_{X0}\cos\theta - H_{Y0}\sin\theta. \quad (6)$$

After studying the preliminary experimental data, we found that the results can be better fit with a "modified S-W model." This model introduces two additional degrees of freedom: these two parameters allow one axis of the asteroid to be longer than the other (as mentioned before, this has been repeatedly observed in prior studies) and also permit a nonperpendicular alignment (skew) of the two "points" of the asteroid:

$$H(\theta) = [L_X\cos^{2/3}(\theta - \theta_K - \theta_T) + L_Y\sin^{2/3}(\theta - \theta_K)]^{-3/2} - H_{X0}\cos\theta - H_{Y0}\sin\theta, \quad (7)$$

where $L_X^{-2/3}$ and $L_Y^{-2/3}$ are equal to the half-lengths of the asteroid along the directions parallel and perpendicular to the anisotropy axis, and the nonperpendicularity of the two asteroid axes is given by θ_T. The solid curve in Fig. 4 represents the curve described by Eq. (7) that best fits the experimental data. It is important to note that this equation cannot be deduced from any known free energy relation; it has been implemented purely in reaction to the experimental results. The issue of asteroid "skew" is the subject of continuing study.

VI. RESULTS

For the initial study, we selected 29 out of a total of 80 junctions on the wafer. The selected junctions chosen were those judged to have more ideal remnant resistance curves

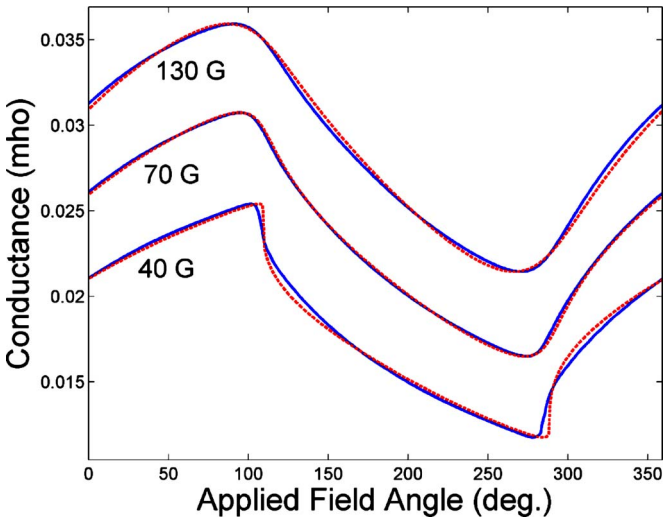

FIG. 5. (Color online) Experimental data (solid lines) and theoretical fitting results (dashed lines) for a set of three circle curves (taken at 40, 70, and 130 G) taken on a representative MTJ element. All fits are made using a single set of junction parameters.

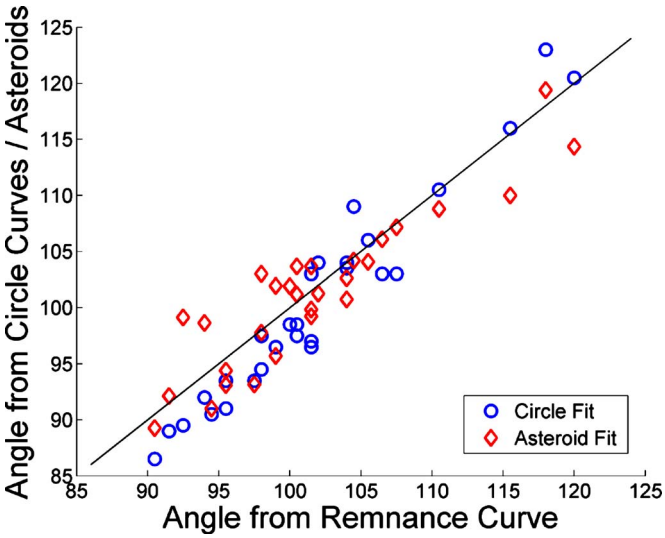

FIG. 6. (Color online) Comparison of the measured anisotropy angles obtained from remnant resistance curves (*x*-axis), asteroid measurements (open diamonds), and circle curve fits (open circles).

(and, therefore, a more S-W-like behavior). For these we have measured a remnant curve, circle curves at 10 G intervals from 30 to 130 G, and angular asteroids. Figure 5 shows three experimental circle curves that were measured for one particular MTJ sample, along with the best-fit curves obtained from fitting to the S-W model as explained above. It is seen that the circle curves deviate more from a pure cosine for weaker applied fields, as the effects of the free layer anisotropy become more pronounced in comparison to the applied field strength.

The free layer anisotropy direction (θ_K) of each junction is the parameter that is perhaps the most important to measure accurately. From these three measurement techniques (asteroid, remnant curves, circle curves), we obtained three independent measures of the anisotropy orientation of each sample. A comparison of the results for θ_K from the three different methods is shown in Fig. 6; it can be seen that there is excellent agreement between all methods.

As a test of the usefulness of the parameters that were extracted from the circle curve data, we have used these parameters to predict the theoretical transfer curves taken at different sweep angles. These predicted curves are shown, along with the actual experimental results, in Fig. 7. It should be emphasized that the theoretical curves contained in this plot were made purely based on the parameters extracted from the circle curve data, with no additional fitting or optimization, and without the need to measure the actual transfer curves themselves. The excellent agreement between theoretical predictions and the data shows that the parameters extracted from the circle curve fits can be used to accurately predict the junction behavior in an arbitrary two-dimensional applied field.

To further understand the capabilities of the circle curve measurement, we measured three circle curves (at 40, 70, and 130 G) for all junctions on this wafer. These measurements took about 2–4 min per junction and could be made much faster (~5–10 s) with some minor upgrades to the measurement apparatus. The obtained anisotropy (θ_K) and exchange bias (θ_E) directions are shown as a function of the position on the wafer in Fig. 8. It can be seen that there is a substantial difference in the two angles. For comparison, we also conducted a similar analysis for all the devices on another wafer, with a similar (but not identical) layer structure, which had been subjected to a standard one-step annealing process.[23] The extracted directions of the free layer anisotropy as well as the exchange bias for this sample are shown in Fig. 9. As expected, the results from this wafer confirm that the free layer anisotropy and exchange bias directions were very similar for most samples.

VII. DISCUSSION

As explained above, we set forth to measure six parameters. The extracted anisotropy strength (H_k) for each sample

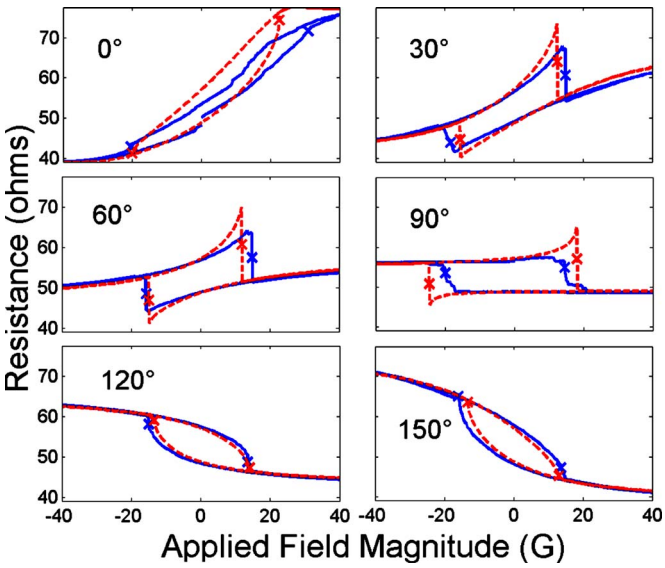

FIG. 7. (Color online) Comparison between measured transfer curves taken at different field sweep angles (solid lines), with simulated transfer curves based on the extracted circle curve parameters (dashed lines). This plot shows that the circle curve results alone can accurately predict junction behavior in arbitrary applied fields.

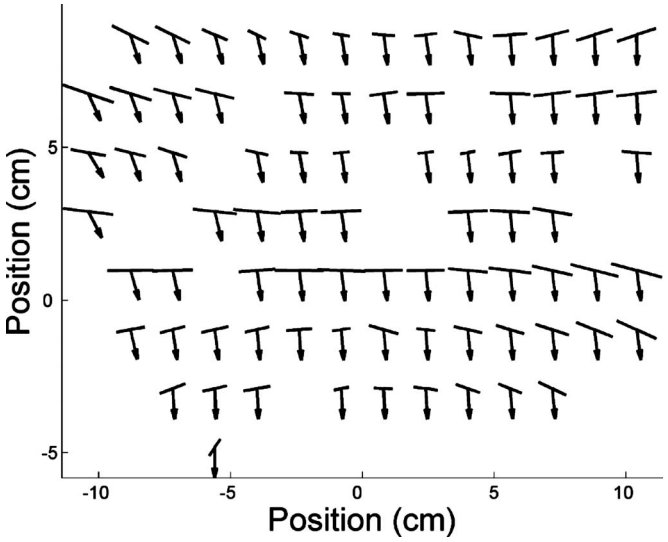

FIG. 8. Plot showing the distribution of junction anisotropy angle and pinned layer direction as a function of wafer position for the twice-annealed sample. The arrows indicate the pinned layer orientation, while the length and orientation of the solid lines indicate the strength and direction of the sample anisotropy, respectively.

is represented graphically by the length of the lines in Figs. 8 and 9. Due to the relatively large size of the junctions, it is reasonable to assume that magnetic coupling between adjacent domains has a minimal effect on the results for large applied fields. This is backed up by the fact that circle curves measured for both clockwise and counterclockwise sweep directions give identical results. Since we are modeling the junction as an ideal S-W particle, we do not take into account any dispersion of the anisotropy direction or magnitude. If we instead assume that the junction can be represented as a collection of noninteracting S-W free particles, any dispersion of anisotropy strength or direction has an averaging effect on the circle curve, making it appear more cosinelike. We also simulated a theoretical junction with a Gaussian distribution of anisotropy. For this sample, our single-domain assumption will still allow a determination of the correct (average) anisotropy direction, but will underestimate the average anisotropy magnitude. Additionally, if circle curves taken with different magnitudes are analyzed, different anisotropy magnitudes will be obtained. In practice, we have observed that this anisotropy dispersion is the most common reason for problems with fitting a set of circle curves to a universal set of junction parameters. Because of this, it is important to measure circle curves for a wide range of magnitudes when conducting such a fit. If one set of parameters fits the data reasonably well, it is an indication that the junction has minimal dispersion in the free layer anisotropy parameters (H_K, θ_K), and that the junction can be safely approximated by a single particle.

The anisotropy magnitude H_k is difficult to determine from the asteroid data. In almost all experimental asteroids, the two axes have different lengths due to the aforementioned stretching effect. Therefore, it is hard to say which axis, if either, can be used as a reliable measure of the device anisotropy. It is known that the length of the measured asteroid along the anisotropy direction is usually truncated as a

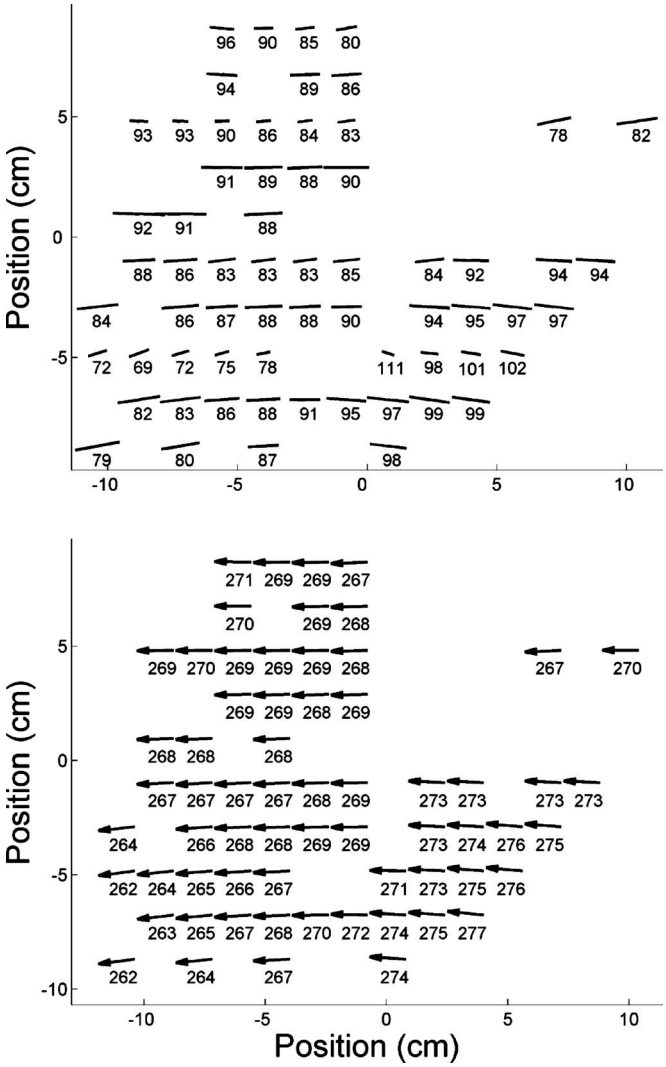

FIG. 9. (a) Plot of the positional distribution of junction anisotropy angle and magnitude for the sample with standard annealing. The numbers below each line show the anisotropy angle in degrees, while the length of each line is proportional to the anisotropy strength. (b) Distribution of the extracted pinned layer direction for the same sample, as a function of wafer position.

result of noncoherent switching processes (domain-wall motion or nucleation).[14,16,17] The length of the perpendicular axis is more likely to represent the true anisotropy strength, but this axis is often very difficult to measure accurately because of the lack of distinct switching events in this part of the asteroid. The anisotropy magnitudes that were extracted from the circle curve fits fell in between the values estimated from the lengths of the two asteroid axes in nearly all cases; however, this range of values was often quite large.

Since the remnant resistance curves indicated very low dispersion (standard deviation $<10°$ for all junctions) and the universal fits agreed reasonably well with the circle curve data for all field strengths, we can assume that the results are fairly accurate. However, more work needs to be done to determine an optimal method for measuring the anisotropy strength.

The circle curves seem capable of very accurately determining both the free layer anisotropy and exchange bias angles (θ_K and θ_E). The anisotropy angle extracted from the circle curves correlates very well with the results from both

TABLE I. A summary of the strengths and weaknesses of the different magnetic characterization methods.

Characterization technique	Relative speed	Best for…	Weaknesses
Fixed-bias asteroid	Slower	H_{0X} and H_{0Y}	No info on θ_E, H_E, MR, R_P; prior knowledge of θ_E can be required
Fixed-angle asteroid	Slower	H_K, θ_K	No info on θ_E, H_E, MR, R_P
Circle transfer curves	Fastest	θ_E, H_E, MR, and R_P	Fitting difficult without prior info or guesses, assumes single domain
Remnant resistance curves	Faster	θ_K, dispersion of θ_K	No info on θ_E, H_E, MR, R_P

the remnant curve and asteroids, as seen in Fig. 6, and is in better agreement with the remnant curve anisotropy data than the asteroids (with an average error of 2.6°). In this figure, the asteroid anisotropy angle is assumed to lie perpendicular to the fitted angle of the asteroid's stretched axis. Data calculated in this way are much more correlated with results from the other methods (average errors of 3.2° and 4.2° with respect to the remnant curve and circle curve data, respectively) than were data calculated from the angle of the asteroid's short axis (7.0° and 8.7°, respectively). We therefore conclude that the former method is a better measure of the free layer's anisotropy direction θ_K.

It is also not hard to understand why the circle curve can accurately determine the pinned layer direction, because a change in the pinned layer's orientation will cause a relative phase change in the circle curves. For large enough applied field magnitudes (H_A), the pinned layer direction can be roughly estimated by simply finding the angle of minimum resistance, as long as $H_E \gg H_A$. The pinned layer angle, seen in Figs. 8 and 9, varies smoothly across both wafers. Therefore, we believe that these values are accurate to within a few degrees.

The remaining three parameters (H_{0X}, H_{0Y}, and H_E) only have small perturbative effects on the circle curves if $H_E \gg H_A$ and H_{0X}, $H_{0Y} \ll H_A$. The pinned layer exchange strengths (H_E), which were extracted for devices on this wafer, were quite strong and consistent (averaging 2.5 kG), which agrees with earlier magnetometry data. Therefore, the pinned layer orientation was essentially constant throughout all the measurements ($|\theta_E - \theta_P| < 3°$). Additionally, it was estimated from the circle curve fits that the offset fields were quite small (<3 G) for all the devices on the wafer. This result was corroborated by the asteroid measurements, which have been shown to be an excellent way to calculate the strength of the offset fields.

VIII. CONCLUSIONS

As indicated by Fig. 8, the two-step annealing process had some success in moving the pinned layer orientation away from the free layer's anisotropy axis. Although no junction showed perfect perpendicular alignment of these two axes, this annealing process clearly was able to substantially realign the pinned layer orientation without creating major changes in the anisotropy of the free layer. As a result, these devices exhibited substantially more linear low-field transfer curves, improving their sensor characteristics. These devices also required correspondingly less applied hard-axis field to remove the magnetic hysteresis, as compared with devices that underwent a single annealing process.

A summary of the different measurement techniques, along with their strengths and weaknesses, is shown in Table I. Of all the existing transport measurement techniques, we believe that circle curves are perhaps the best way to evaluate the anisotropy angle and magnitude of individual MTJ elements, and to determine the exchange bias direction. Circle curves are especially useful for studying devices where the exchange bias and anisotropy orientations are not parallel, because asteroid measurements become difficult to interpret in this case. For MTJs with substantial offset fields, the two additional parameters make the process of fitting the circle curves somewhat more complicated. In this case, we feel that the best approach might be to initially use an asteroid measurement to determine the offset fields, and then take circle curve data, which is offset from the field space origin to cancel out the effects of these fields.

We also believe that remnant resistance curves are an excellent way to obtain more information about the orientation and dispersion of the free layer anisotropy. These measurements can also be used as a quantitative way to understand how closely a particular MTJ conforms to the Stoner-Wohlfarth assumption of single particle behavior with a uniaxial anisotropy. Therefore, measuring the remnant curve is perhaps the best way to understand whether the simple S-W model can adequately describe the magnetic behavior of a given sample.

We believe that these results show that circle curves can be used as a new and complementary tool to existing characterization methods for groups attempting to understand the behavior of MTJ (or similar) devices. Both circle curves and remnant resistance curves require no additional hardware beyond what is needed for standard asteroid measurements, and these methods can be very useful in place of—or in addition to—standard asteroid methods. In general, each type of measurement has its own strengths and weaknesses, and the use of multiple methods in conjunction can give a far more comprehensive picture of MTJ behavior than can any one technique.

ACKNOWLEDGMENTS

This work was supported at Micro Magnetics by the National Science Foundation (NSF) Small Business Innovation Research Awards No. 0522160 and No. 0610712, and at Brown by NSF Grant No. DMR-0605966 (Brown). We also gratefully acknowledge partial support from JHU MRSEC (NSF Grant No. DMR-0520491.

[1]J. S. Moodera, L. R. Kinder, T. M. Wong, and R. Meservey, Phys. Rev. Lett. **74**, 3273 (1995).
[2]T. Miyazaki and N. Tezuka, J. Magn. Magn. Mater. **139**, L231 (1995).
[3]W. J. Gallagher, S. S. P. Parkin, Y. Lu, X. P. Bian, A. Marley, K. P. Roche, R. A. Altman, S. A. Rishton, C. Jahnes, T. M. Shaw, and G. Xiao, J. Appl. Phys. **81**, 3741 (1997).
[4]S. S. P. Parkin, K. P. Roche, M. G. Samant, P. M. Rice, R. B. Beyers, R. E. Scheuerlein, E. O. Sullivan, S. L. Brown, J. Bucchignano, D. W. Abraham, Y. Lu, M. Rooks, R. L. Trouilloud, R. A. Wanner, and W. J. Gallagher, J. Appl. Phys. **85**, 5828 (1999).
[5]X. Liu, C. Ren, and G. Xiao, J. Appl. Phys. **92**, 4722 (2002).
[6]D. Song, J. Nowak, R. Larson, P. Kolbo, and R. Chellew, IEEE Trans. Magn. **36**, 2545 (2000).
[7]S. Yuasa, T. Nagahama, A. Fukushima, Y. Suzuki, and K. Ando, Nat. Mater. **3**, 868 (2004).
[8]S. S. P. Parkin, C. Kaiser, A. Panchula, P. M. Rice, B. Hughes, M. Samant, and S.-H. Yang, Nat. Mater. **3**, 862 (2004).
[9]W. Shen, D. Mazumdar, X. Zou, X. Liu, B. D. Schrag, and G. Xiao, Appl. Phys. Lett. **88**, 182508 (2006).
[10]M. Tondra, J. Daughton, C. Nordman, D. Wang, and J. Taylor, J. Appl. Phys. **87**, 4679 (2000).
[11]Y. Lu, X. W. Li, G. Q. Gong, G. Xiao, A. Gupta, P. Lecoeur, J. Z. Sun, Y. Y. Wang, and V. P. Dravid, Phys. Rev. B **54**, R8357 (1996).
[12]D. Lacour, H. Jaffres, F. Nguyen Van Dau, F. Petroff, A. Vaures, and J. Humbert, J. Appl. Phys. **91**, 4655 (2002).
[13]B. D. Schrag, A. Anguelouch, G. Xiao, P. Trouilloud, Y. Lu, W. J. Gallagher, and S. S. Parkin, J. Appl. Phys. **87**, 4682 (2000).
[14]A. Anguelouch, B. D. Schrag, G. Xiao, Y. Lu, P. L. Trouilloud, R. A. Wanner, and W. J. Gallagher, Appl. Phys. Lett. **76**, 622 (2000).
[15]U. K. Klostermann, R. Kinder, G. Bayreuther, M. Ruhrig, G. Rupp, and J. Wecker, J. Magn. Magn. Mater. **240**, 305 (2002).
[16]C. Appino, J. Magn. Magn. Mater. **290-291**, 471 (2005).
[17]Y. Lu, P. L. Trouilloud, D. W. Abraham, R. Koch, J. Slonczewski, S. Brown, J. Bucchignano, E. O'Sullivan, R. A. Wanner, W. J. Gallagher, and S. S. P. Parkin, J. Appl. Phys. **85**, 5267 (1999).
[18]C. Kim, D. Y. Kim, D. G. Hwang, S. S. Lee, and C. O. Kim, J. Magn. Magn. Mater. **239**, 176 (2002).
[19]S. Shtrikman and D. Treves, J. Appl. Phys. **31**, S58 (1960).
[20]R. Iglesias and H. Rubio, Phys. Rev. B **56**, 2605 (1997).
[21]E. C. Stoner and E. P. Wohlfarth, Philos. Trans. R. Soc. London, Ser. A **240**, 599 (1948).
[22]J. W. Harrell, Y. Yu, Y. Ye, J. P. Parakka, D. E. Nikles, and H. G. Zolla, J. Appl. Phys. **81**, 3800 (1997).
[23]X. Liu and G. Xiao, J. Appl. Phys. **94**, 6218 (2003).